Ph.D. Thesis, Faculty of Science,
University of the Witwatersrand, Johannesburg

Imaging the African Superplume -

Upper Mantle, Tomography and Moment Tensor

by

Martin Barend Christopher BRANDT

DECLARATION

I hereby declare that this thesis is my own original work, unless explicitly stated in the Summary and Introduction. This thesis is being submitted towards the fulfilment of the requirements for the degree of Doctor of Philosophy at the Faculty of Science, University of the Witwatersrand, Johannesburg. This thesis has not been submitted towards a degree or examination at any other University or Institution of Higher Education.

Signed at Pretoria at the Council for Geoscience on the 14th of May 2012.

Martin Barend Christopher BRANDT

Abstract

Brandt, Martin B.C. 2011. Imaging the African Superplume – Upper mantle, Tomography and Moment tensor. *Ph.D. thesis*, Faculty of Science, University of the Witwatersrand, Johannesburg, South Africa.

The African Superplume, African Superswell and East African Rift System are amongst the most prominent geophysical features on Earth, but the structure, evolution and interaction between these features is controversial. In my thesis I conducted a range of investigations in an effort to better understand these issues. The thesis presents the investigations into the structure and expressions of these features. These include:
(I) A study of the upper mantle shear velocity structure beneath southern Africa to investigate the source of the buoyancy that has powered the Superswell;
(II) Statistical hypothesis testing of middle-mantle shear velocity tomographic models to evaluate evidence for links between the Superplume and low velocity features in/near the transition zone; and
(III) Computation of three new regional moment tensors for South Africa to assess crustal stress in the Kalahari craton, and its link with mantle structure and dynamics.

Waveform data were obtained for the study on the upper mantle shear velocity structure and the moment tensor inversions from the Southern African Seismic Experiment Kaapvaal craton array. For the statistical hypothesis testing on global tomography images, new travel-time data from both global and AfricaArray stations were added to Grand's global shear velocity data set.

The principal findings of this study are summarized below.

I. The upper mantle shear velocity structure beneath the Kalahari craton is similar to that of other shields, except for slightly slower velocities from 110–220 km depth. The difference may be due to higher temperatures or a decrease in magnesium number (Mg#). If the slower velocities in the deep lithosphere are due solely to a temperature anomaly, then slightly less than half of the unusually high elevation of the Kalahari craton can be explained by shallow buoyancy from a depleted hot lithosphere. Decreasing the Mg# of the lower lithosphere would increase density and counteract higher temperatures. If an excess temperature of 90 K over a 110 km depth range and a corresponding decrease in Mg# of -2 between the Kalahari and the other cratons are assumed, this would match the seismic velocity difference but would result in essentially no buoyancy difference. We conclude that the high elevation of the Kalahari craton can only be partially supported by shallow mantle buoyancy and must have a deeper source.

We determined a thickness of 250±30 km for the mantle transition zone below eastern southern Africa, which is similar to the global average, but the corresponding velocity gradient is less steep than in standard global models (PREM and IASP91). Velocity jumps of 0.16±0.1 km/s (eastern) and 0.21±0.1 km/s (central) across the 410 km discontinuity were found. Our results indicate a thermal or chemical anomaly in the mantle transition zone, but this cannot be quantified due to uncertainty.

II. Statistical hypothesis testing on our global tomography images indicated that the African Superplume rises from the core-mantle boundary to at least 1150 km depth, and the upper mantle slow-velocity anomaly extends from the base of the lithosphere to below the mantle transition zone. The model that links the African Superplume with the slow-velocity anomaly in the upper mantle under eastern Africa has an equal probability to an alternative hypothesis with a thin slow-velocity "obstruction zone" at 850 to 1000 km depth.

III. Finally, we calculated three regional moment tensors for South Africa and made progress towards resolving the discrepancy between the local and moment magnitudes we observe for the region. Moment tensors/focal mechanisms in southern Africa change from normal faulting (extension) in the northeast near the East African Rift to strike-slip faulting in the southwest. This confirms previous studies stating that not only eastern Africa, but also southern Africa is being actively uplifted by lithospheric modification at its base and/or the African Superplume.

Papers included in the thesis

This thesis is based on the following papers, which are referred to in the text by their Roman numerals:

I. Brandt, M.B.C., S.P. Grand, A.A. Nyblade and P.H.G.M. Dirks (2011). Upper mantle seismic structure beneath Southern Africa: Constraints on the buoyancy supporting the African Superswell. *Pure and Applied Geophysics*, doi:10.1007/s00024-011-0361-8.

   This article was presented at the 10th Biennial South African Geophysical Association Conference & Exhibition, 22–26 October 2007, Wild Coast Sun, South Africa, and the International Association of Seismology and Physics of the Earth's Interior, 11–16 January 2009, Cape Town, South Africa.

II. Brandt, M.B.C. and S.P. Grand. Middle mantle seismic structure of the African Superplume. *Submitted to Pure and Applied Geophysics*.

III. Brandt, M.B.C. and I. Saunders (2011). New regional moment tensors in South Africa. *Seismological Research Letters*, 82(1), 7–18, doi:10.1785/gssrl.82.1.7.

Contents

1. Introduction

The African Superplume, African Superswell and East African Rift System are amongst the most prominent geophysical features on Earth, but the structure, evolution and interaction between these features is controversial. Seismology is the study of earthquakes, specifically the generation, propagation and recording of elastic waves through the Earth, the sources that produce these waves, and the effect the waves have on the surface and man-made structures (e.g., Lay and Wallace, 1995). Classical seismology uses waves from individual or multiple earthquakes to determine the structure of the Earth or derive the source mechanism (e.g. moment tensor inversions). However, in southern and eastern Africa, the study of earthquakes and Earth structure is influenced by the single massive mantle structure, called the African Superplume (e.g., Gurnis *et al*., 2000). This global structure consists of a large-scale, slow-shear-velocity anomaly beneath the African plate that extends from the core–mantle boundary to about 1500 km above the core–mantle boundary under eastern Africa (e.g., Simmons *et al*., 2007). Various global tomographic images show shear velocities up to 3% slower than that of the average mantle for the Superplume at depth (e.g., Grand, 2002).

One of the most studied subjects regarding the African Superplume is the upper mantle velocity structure underneath southern Africa. Even though there is only tenuous evidence of a connection between the imaged lower mantle plume and the lithospheric mantle, upper mantle buoyant support for the high topography has been suggested by researchers such as Priestly (1999), Li and Burke (2006) and Wang *et al*. (2008), who all found a strong S-wave low-velocity zone (LVZ). Other researchers, e.g., Saltzer (2002) and Larson *et al*. (2006), found little evidence for such a proposed LVZ. Hence it is still not clear whether southern Africa is underlain by an upper mantle that is anomalously seismically slow and buoyant. Lithgow-Bertollini and Silver (1998) proposed an alternative hypothesis to explain the uplift of southern Africa, i.e. dynamic forces produced by viscous flow from the African Superplume.

The mantle under southern Africa between 410 and 670 km depth has been investigated before using receiver functions. However, there was little evidence for an unusual transition zone (e.g., Gao *et al*., 2002) that would indicate a thermal anomaly within the deep upper mantle (e.g., Bina and Helffrich, 1994).

Imaging the upper mantle velocity structure has been attempted with both body waves and surface waves (e.g., Wang *et al*., 2008; Saltzer, 2002). We extended Wang *et al*.'s (2008) study with a different approach by matching the waveform data to derive an upper mantle velocity structure (Paper I). We also made use of recently published studies that infer, from an interpretation of garnet xenocrysts in kimberlites, the compositional structure and thermal state of the lithospheric mantle beneath the Kalahari craton. This information was applied to estimate the lithospheric buoyancy from a purely thermal state, a purely compositional state, and a combination of both states. We also investigated the depths of the 410 and 660 km discontinuities, as well as the velocity jumps across the 410 km discontinuity (Paper I).

Another frequently studied subject is the middle mantle seismic velocity structure beneath eastern Africa. In the upper mantle a 200–400 km wide slow-velocity zone beneath the eastern branch of the East African Rift extends into, but not necessarily through, the mantle transition zone. Shear-velocity reduction greater than 3% extends to between 100 and 150 km depth and velocity reductions of ~2.5% persist to at least 400 km depth (Nyblade *et al*., 2000). Ritsema *et al*. (1999) proposed that the African Superplume extends from the core–mantle boundary under southern Africa into the slow-velocity anomaly in the upper mantle under eastern Africa.

We obtained new travel-time data from global and AfricaArray stations. Thereafter, we derived Grand's (2002) updated global tomographic model. The tomographic model images indicate slow shear velocities associated with the East African Rift from the surface to a depth of at least 325 km. At greater depth, several slow-velocity arms extend westwards and southwards from the Rift towards the West Africa craton, where, at greater depths, these arms join and link with the top of the African Superplume (Begg *et al*., 2009). We undertook statistical hypothesis testing to compare the validity of the model in which the upper slow-velocity anomaly is linked in a complex way to the Superplume, with an alternative model with an "obstruction" between the lower African Superplume and upper slow-velocity anomaly (Paper II). Such an "obstruction" could be a thermal boundary layer separating two convecting regions in the mantle (Montelli *et al*., 2004).

There have been very few studies of earthquake moment tensors and fault mechanisms in southern Africa owing to moderate tectonic seismicity and, until recently, few broadband seismometers in the region. Due to the lack of moment tensors for southern Africa, no moment magnitude scale has yet been implemented for the region and little is known about the regional seismotectonics. Moment tensor/fault plane solutions vary from normal (extension in the northeast) to strike slip (in the southwest). Southern Africa is being actively uplifted at a rate of at least 8 to 17 m/Myr (e.g., Gurnis *et al*., 2000). This has led scientists (e.g., Fan and Wallace, 1995) to hypothesise that the crustal stresses in northeastern South Africa may be related to uplift associated with buoyancy in the upper mantle and/or the African Superplume. We derived three new regional moment tensors with a time-domain waveform fitting technique and also calculated moment magnitudes (Paper III). Our results confirm the hypothesis of active uplift.

2. The African Superplume

The African Superplume is both one of the most prominent and one of the most enigmatic features of the Earth's mantle. Underlying much of the southern African subcontinent, it is characterised by seismic wave velocities that are slower than other structures in the Earth's lower mantle. While it is still uncertain exactly what the Superplume is, most researchers today think it to be a giant upwelling of mantle material. The Superplume also lies beneath an area with an anomalously high topography, suggesting land surface uplift, and hence a geodynamic relationship between the Superplume and the formation of plateaus and rift valleys in eastern and southern Africa has been postulated (e.g., Lithgow-Bertelloni and Silver, 1998; Ritsema *et al.*, 1999; Gurnis *et al.*, 2000; Simmons *et al.*, 2007; Moucha and Forte, 2011).

The velocity structure of the Superplume has been mapped with detailed global tomography images. At first it was mapped with global P-waves and found to be close to the average compressional velocity (e.g., Dziewonski, 1984). However, the shear wave velocity is up to 3% slower than that of the average mantle (e.g., Ritsema *et al.*, 1998; Ritsema *et al.*, 1999). By the end of the 20^{th} century, this velocity anomaly became known as the ''African Superplume'' (e.g., Gurnis *et al.*, 2000). The large-scale upward extension rises from its base under southern Africa into the mid-mantle, tilting towards eastern Africa, to at least 1500 km above the core–mantle boundary (Figure 2.1). However, the images do not show a connection from the lower mantle to the lithospheric mantle, except perhaps under the East African Rift, where a 200 to 400 km wide zone of slow velocities is seen beneath the eastern branch of the Rift (e.g., Nyblade *et al.*, 2000). In the Rift, the continental crust is in the early stages of being split apart by horizontal motions (e.g., Moucha and Forte, 2011).

The seismic shear wave velocities inside the structure are slower than normal, indicating that the Superplume may be hotter than the surrounding mantle and/or may include chemical changes (e.g., Simmons *et al.*, 2007). Detailed waveform analyses have revealed that the plume possesses a ridge-like morphology (i.e., like a chain of mountains that form a continuous elevated crest) and abrupt wave speed reductions near its boundaries (Figure 2.1). Slow seismic shear wave speeds may indicate high temperatures, but the morphology and abrupt velocity jumps associated with the structure cannot be easily attributed to temperature variations alone, implying potential chemical changes. This hypothesised chemical component means that at least part of the Superplume is denser than the surrounding mantle, which slows its rise upwards (e.g., Ni *et al.*, 2002; 2005). A study into the Earth's orientation relative to its spin axis determined from the nonhydrostatic inertia tensor (caused by large slow shear velocity anomalies in the mantle) has led Steinberger and Torsvik (2010) to suggest a longevity for the Superplume of more than ~50Ma.

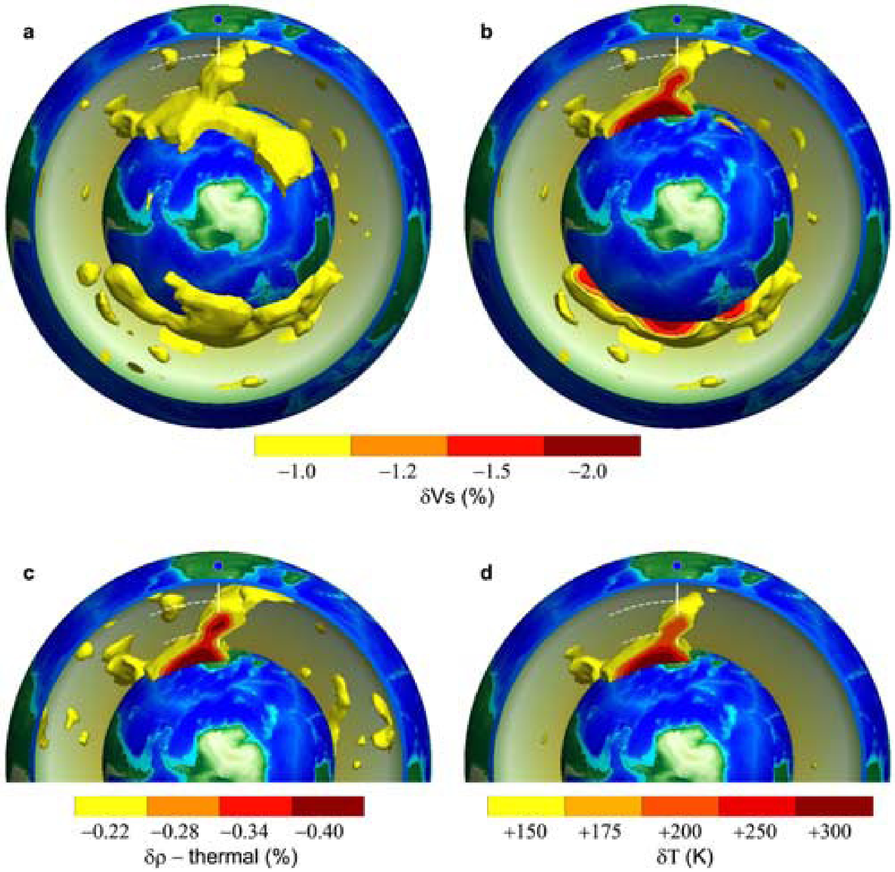

Figure 2.1. Isocontours of the velocity, thermally induced density and temperature fields within the African Superplume region. The earth is sliced open and the surface topography is projected onto the core mantle boundary for perspective. The white vertical line is for spatial reference and intersects the southern African continent at 25° S latitude and 25° E longitude. The dashed lines correspond to 1000 and 2000 km depths. (a) Shear-wave velocity perturbation field determined by simultaneous inversion of seismic and geodynamic data. (b) Internal view of the shear-wave perturbation field. (c) Internal view of the thermally induced density field found by converting the velocity field with a velocity-density relationship. (d) Temperature variations. (After Figure 2 in Simmons* et al.*, 2007).

The African Superplume may uplift the surface of southern and eastern Africa via a large-scale, positively buoyant structure within the mid-lower mantle that causes viscous flow (e.g., Gurnis *et al*., 2000). If the Superplume is connected to the lithospheric mantle under the East African Rift, it would play a direct role in the region's volcanism and rifting. However, directly above the Superplume itself, in southern Africa, there is no volcanism at all, yet the topography is elevated to an unusual height. The high topography cannot be accounted for by a variation in crustal thickness or normal plate cooling. The subcontinent is rimmed by the Great Escarpment, which extends for almost 3000 km around the southern margin of Africa, separating a vast interior plateau, with 500 m of positive residual elevation, from a narrow coastal strip. The elevated topography extends from southern Africa through the East African Rift and continues into the southeastern Atlantic Ocean basin southwest of the African continent. The entire region from the South Atlantic to eastern Africa has been named the African Superswell (e.g., Partridge and Maud, 1987; Nyblade and Robinson, 1994; Nyblade and Langston, 1998).

The mantle density and viscosity can be constrained by the dynamic topography uplift rate and this may be used to unravel the structure, temperature and composition of the Superplume (Lithgow-Bertelloni and Silver, 1998; Gurnis *et al*., 2000). If the Superplume was only due to a temperature anomaly, then the residual elevation would be higher than it is today, but the observed topography is better fit by a model where the Superplume is due to both thermal and compositional anomalies (e.g., Simmons *et al*., 2007).

3. Data

3.1 SASE Kaapvaal craton array

The Southern African Seismic Experiment (SASE) Kaapvaal craton array consisted of 55 broadband REFTEK/STS2 instruments from IRIS/PASSCAL with 120 s eigen periods deployed at 81 sites between April 1997 and July 1999 (Figure 3.1). The Kaapvaal array seismometers were arranged along a roughly NE–SW axis in southern Africa in the countries of South Africa, Botswana and Zimbabwe. The SASE data, continuously recorded data at 20 samples/s, were supplemented by data from three global digital stations in the region of the array (e.g., James *et al.*, 2001). The data are available freely to all users and I obtained it from the IRIS PASSCAL data centre.

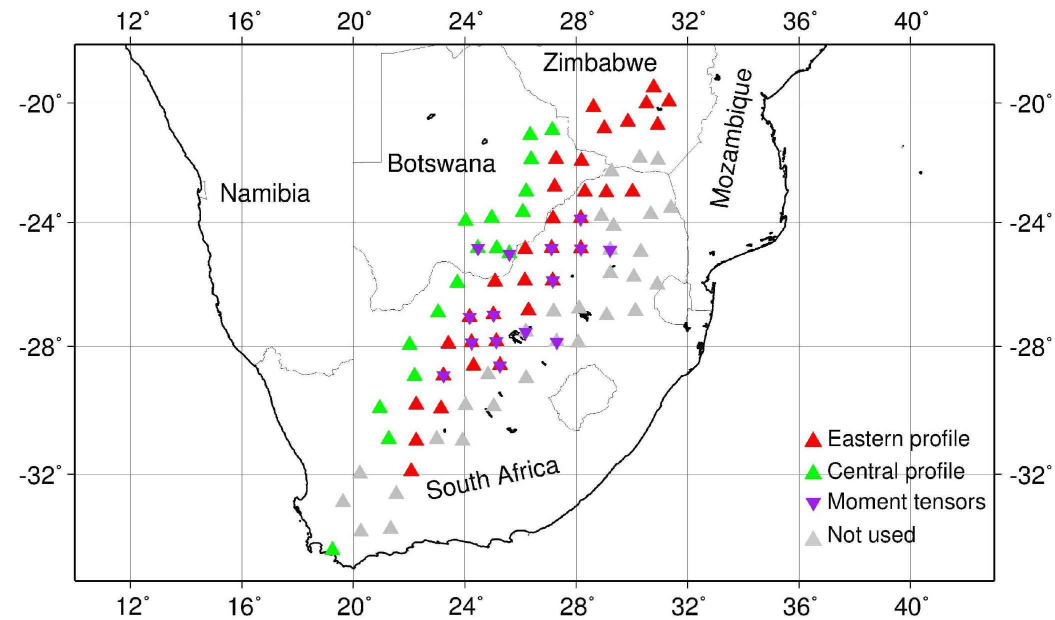

Figure 3.1. Station map of the Kaapvaal Southern African Seismic Experiment. Red and green triangles indicate stations of the first deployment used for the Eastern and Central profiles of Paper I, grey triangles show stations of the second deployment, as well as noisy stations from the first deployment at large distances from the earthquake not used. Purple, inverted triangles indicate stations from the first and second deployments to determine the moment tensors in Paper III.

For paper I we used SASE Kaapvaal array seismic waveform data from the stations of the first deployment (Figure 3.1). The waveforms were generated by a shallow M_w=5.9 earthquake located at Lake Tanganyika on 21 September 1997. The SASE Kaapvaal array spanned 12.1° to 28.7° in distance from this event and the stations lie approximately along a great circle. This was the only earthquake for the whole deployment period with an appropriate distance and azimuth from the array to map the upper mantle, and with a magnitude large enough for detection by most of the stations.

For Paper III, we used waveform data from three moderate earthquakes with M_w ~4 in South Africa recorded by stations with epicentral distances of less than 400 km (Figure 3.1). These were the only earthquakes for the whole observation period that were recorded by at least five stations with an adequate signal-to-noise ratio.

3.2 Networks used for the global tomography study

To prepare data for the statistical testing of mantle tomography models (Paper II), differences between the times of observed arrivals and those predicted by a one-dimensional starting model (taken from Grand, 1994) were determined for 2600 new S, SS, ScS, SKS and SKKS phases from earthquakes of magnitude 5.8 to 6.6 that occurred between 25 October 2007 and 19 November 2008 (Figure 3.2). These data were added to a set of 41,469 phases that Grand (2002) and Simmons *et al*. (2007) used to produce their global tomography models.

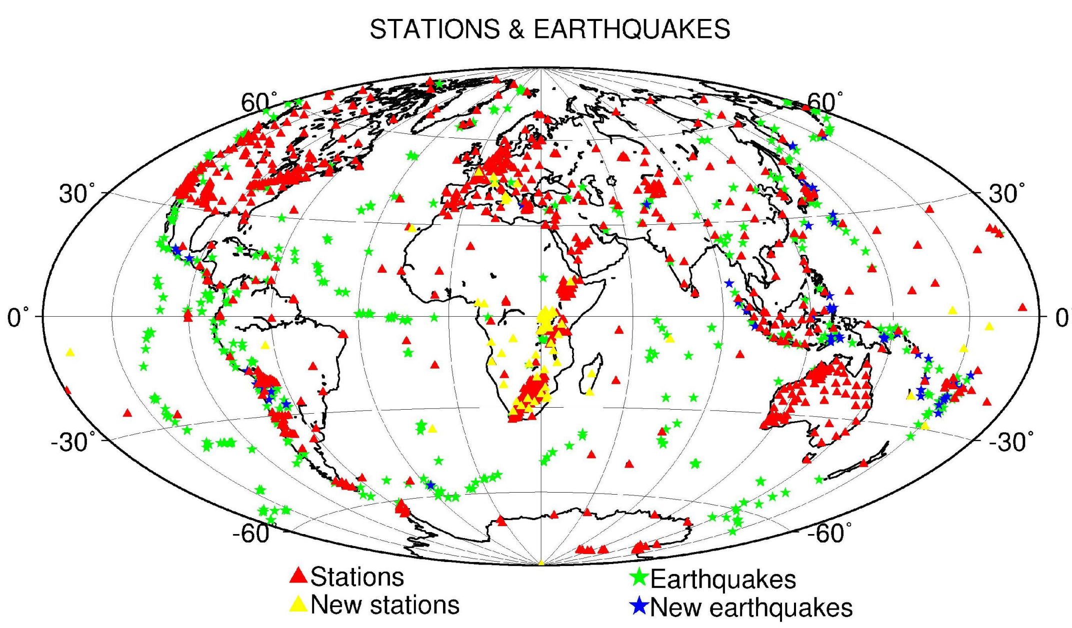

Figure 3.2. Station map of the networks from which phases were added to the global tomography data set. Red and yellow triangles indicate stations used before and stations that contributed new data, respectively. Green and blue stars represent earthquakes used before and new earthquakes, respectively.

These earthquakes were recorded by the networks MEDNET (Istituto Nazionale di Geofisica, Italy), GEOSCOPE (Institut de Physique du Globe de Paris), AfricaArray (Pennsylvania State University, USA, The University of the Witwatersrand, South

Africa, and the South African Council for Geoscience), Global Telemetered Southern Hemisphere Network (USGS Albuquerque Seismological Laboratory, USA), IRIS/IDA (University of California and Scripps Institution of Oceanography, USA) and IRIS/USGS (USGS Albuquerque Seismological Laboratory, USA). These networks all follow open data policies and the data are available upon request for research purposes. Data from all the available stations were added.

To better image the African Superplume, reflected and depth phases (ScS, SKS and SKKS) were included in the tomography data set from upgraded and newly installed African stations. One such example is the phase readings from an earthquake that occurred in Argentina in 2007 and was recorded by stations in southern and eastern Africa (Figure 3.3).

Data from upgraded and new stations were made available to the global tomography data set by AfricaArray, which is an affiliation of organisations/institutions which conduct coupled research/training projects to strengthen scientific capacity in Africa (Figure 3.4) (Nyblade *et al*., 2008). The goal of the first phase of AfricaArray (2005–2007) was to establish a network of 20 to 30 permanent observatories spanning much of southern and eastern Africa. The placement of permanent observatories in many countries was governed by the location of existing seismic stations that have been pledged to AfricaArray. Seismic equipment at many of these stations was upgraded, the data have been formatted uniformly and archived, and access to the data has been streamlined. During the second phase of AfricaArray (2008–2010), the network of permanent observatories was expanded into other parts of Africa, with emphasis on establishing temporary (flexible) networks of seismic stations, with a small station spacing, focused on specific targets of economic, societal or academic interest (e.g., fault systems, sedimentary basins, ultramafic intrusives) (Nyblade *et al*., 2008).

My involvement with seismograph installation/upgrades was limited to the South African National Seismograph Network (SANSN). The SANSN was upgraded by staff in the Seismology Unit (including the author) in 2006 with a government grant to record 24 hours per day with real time data communication by cellphone. Stations were fitted with new extended short period seismometers (30 s) and seven selected stations received broadband (100 s) sensors (Saunders *et al*., 2008). The Council for Geoscience operates one very broad band (120 s) seismograph in the Botanical Gardens next to its head office in Pretoria. In 2006, the Council for Geoscience signed a memorandum of understanding with AfricaArray to pledge data from 10 stations. My responsibility was to provide station and calibration details in the correct format for AfricaArray and ensure that the data were delivered every day.

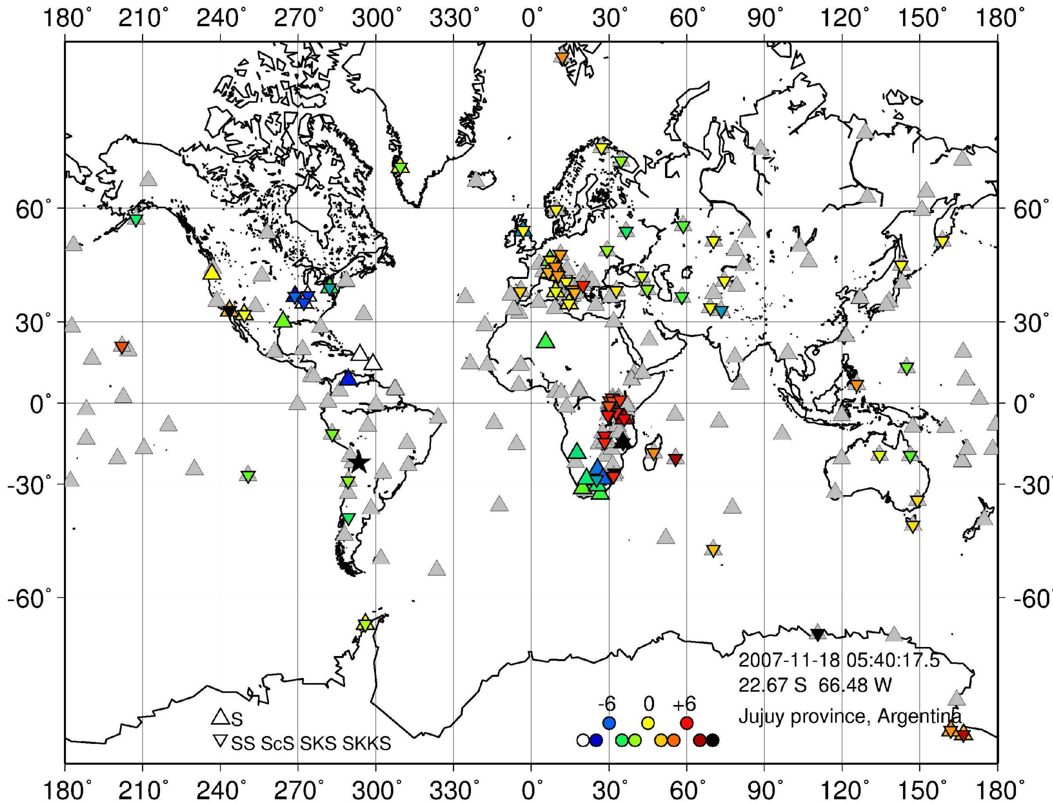

Figure 3.3. Station map of the networks from which phases were added to the global tomography data set for the earthquake that occurred on 2007-11-18. Triangles refer to direct phases (S) and inverse triangles to reflected and depth phases (SS, ScS, SKS and SKKS) that were recorded at that station. The star in Argentina represents the earthquake. Warm colors refer to delayed travel-times and cold colors to early travel-times versus those predicted by a one-dimensional reference model, respectively. Grey triangles represent phases rejected due to poor synthetic to data waveform fits. Note the large, positive travel-time residuals of the depth phases recorded in eastern Africa that travel through the African Superplume in comparison to those with large, negative travel-time residuals recorded in southern Africa.

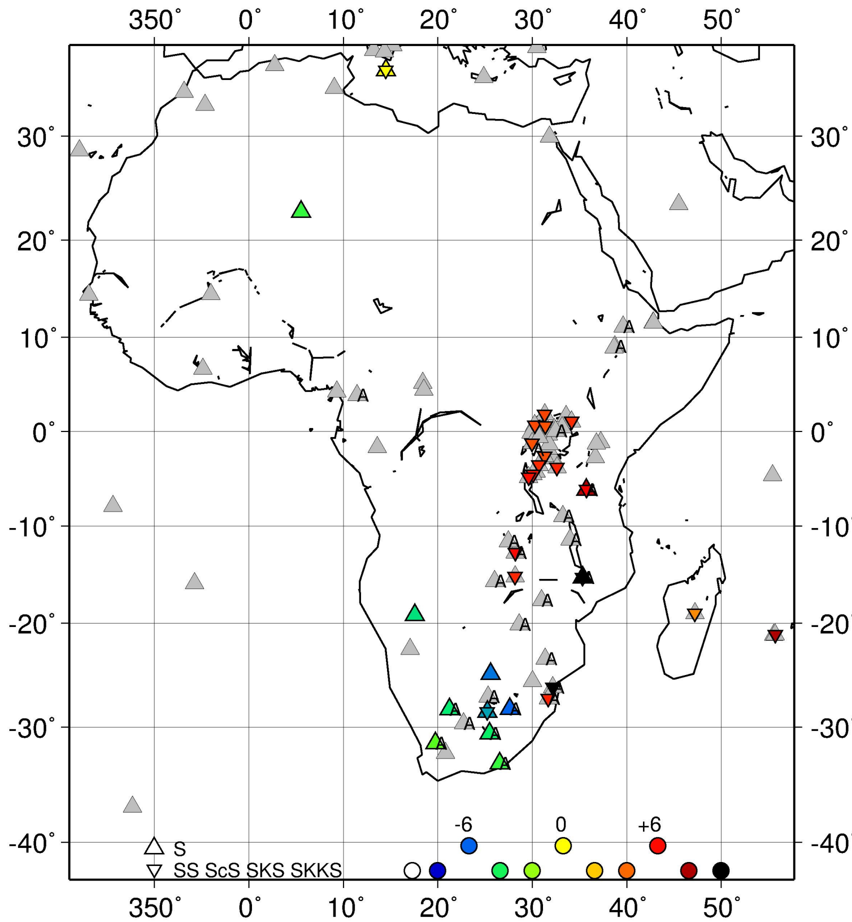

Figure 3.4. Station map of Africa of the networks from which phases were added to the global tomography data set for the earthquake that occurred on 2007-11-18. This is a blow-up of Figure 3.3. Symbols and colors have the same meaning as before. AfricaArray stations operational at the time are labelled with an "A".

4. Paper I: S-velocity seismic structure of the upper mantle

4.1 Work done by the PhD candidate

I derived the upper mantle seismic structure with software provided to me by Dr Eric Matzel, former student of the University of Texas at Austin, and now working at the Lawrence Livermore National Laboratory. The FORTRAN source code was originally written for a SUN workstation and a typical inversion would take about forty minutes to one hour. I adapted the code for a Pentium laptop computer running a LINUX operating system. A typical inversion lasted 10 to 12 hours and hence I completed the modelling overnight.

I obtained the waveform data from the IRIS PASSCAL data centre and obtained the Seismic Analysis Code (SAC) from the IRIS data centre. I completed all the data pre-processing with this software. This included removal of the far noisy stations, band pass filtering, component rotation into transverse (SH) orientation, re-digitising at a lower sample rate, and aligning the synthetics with the data at a reduction velocity. I wrote FORTRAN codes to select windows from the waveform data and wrote SAC macros to display these in graphical format to aid me in identifying the various phases shown in, e.g., the article in Figure 10b. I also completed various Matlab codes to display the graphics in Figures 5 to 13 for interpretation of the results and sensitivity analyses. Afterwards, I prepared the data, modeling and parameter input files, and completed the inversions. It took about one week to perform one complete inversion, together with the sensitivity analysis and all the input file changes.

I wrote the article under the guidance of Prof. Grand, whereas Prof. Nyblade and Prof. Dirks arranged the AfricaArray programme as co-directors. I submitted the manuscript to Pure and Applied Geophysics and afterwards made the reviewer corrections with advice from Prof. Grand.

4.2 Previous models

Upper mantle shear velocity models published by Li and Burke (2006), Priestley (1999) and Wang *et al*. (2008) all have strong LVZs (velocities less than 4.5 km/s between 200 to 300 km depth). In Figure 4.1 we compare these models, as well as surface wave models without a significant LVZ by Saltzer (2002) and Larson *et al*. (2006). The models from Priestly (1999), Larson *et al*. (2006) and Li and Burke (2006) were derived from Rayleigh wave data, whereas Saltzer (2002) used both Rayleigh and Love waves. Wang *et al*. (2008) used only body waves to derive their model. The primary data sets used in the surface wave inversions were Rayleigh wave phase velocities. It is likely that the differences between the SH wave velocity results and those of the mostly Rayleigh wave studies for the shallow mantle above 150 km (see Figure 4.1) are due to the anisotropy, which is included in the PREM model

(Dziewonski and Anderson, 1981). The PREM model is anisotropic for the upper 200 km of the mantle: the SH velocity is faster than the SV velocity; and the SH velocity structure has a strong LVZ, in comparison with the slight LVZ for SV. SH–SV wave anisotropy has been invoked to explain Love-Rayleigh wave discrepancies, although this is not strictly correct since Rayleigh wave velocity also depends on the anisotropic P-wave velocity structure.

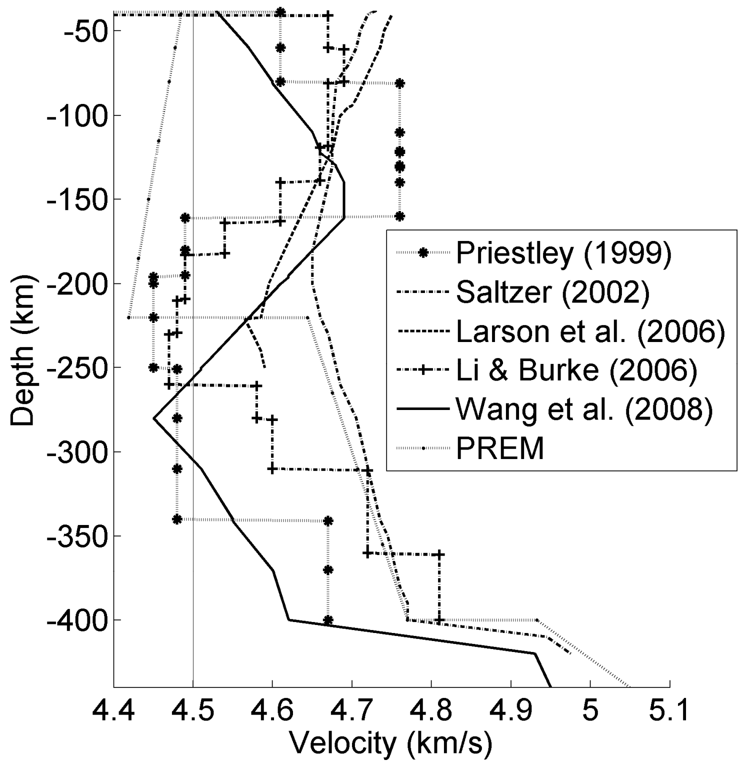

Figure 4.1. Comparison of five upper mantle shear velocity models for southern Africa. Three have strong low-velocity zones. The models from Priestley (1999, Larson* et al. *(2006) and Li and Burke (2006)) were derived from Rayleigh wave data, whereas Saltzer (2002) used both Rayleigh and Love waves. Wang* et al. *(2008) used body waves. PREM refers to the preliminary global reference SH model (Dziewonski and Anderson, 1981).

Observations of shear-wave splitting and surface waves led Silver *et al*. (2004) to conclude that the eastern Kaapvaal shield is almost isotropic. The Shield is flanked by a spatially continuous arc of anisotropic mantle that extends from the western and northwestern Kaapvaal craton, to the Limpopo and Magondi belts, and to the Zimbabwe craton. However, anisotropy has been found to decrease with depth and cannot be resolved below 150 km (Saltzer, 2000). Hence, anisotropy cannot explain the differences between the models with and without a significant LVZ below 200 km.

All surface wave studies for southern Africa prior to 2001 (before results of the SASE PASSCAL Kaapvaal array were published) were based on very few widely spaced stations. The paths analysed include regions that vary from cratons to extensive mobile belts (e.g., Larson *et al*., 2006). Hence, the model by Priestly (1999) could have been influenced by tectonic terranes other than the craton that were traversed by the surface waves. This does, however, not explain different results of surface wave studies after 2001 as they all made use of data from the Kaapvaal craton array. The objective of our research was to investigate these different results. Our approach was to repeat the modelling with the exact same data set, but with a different inversion technique, perform a sensitivity analysis of our result and then compare waveform to synthetics data fit with a previous result. This should provide more insight into the underlying assumptions of the techniques and models, effect of inversion procedures, resolution of the velocity structures and range of valid models. We selected Wang *et al*.'s (2008) body wave velocity model because it is possible to directly compare new results as well as data to synthetic fits.

4.3 Re-modelling Wang *et al*. (2008)

Wang *et al.'s* (2008) data set includes the data used in our study, but their approach was to use a limited number of models to do trial-and-error modelling of the waveforms of triplicated waves. They also used a different frequency band than for this study, namely 1–50 s and not 5–100 s, and a different source origin time. Their models have a high-velocity lid that is 150 km thick, with a strong LVZ beneath. They concluded that the LVZ could have had a low density and thus provided some of the buoyancy supporting the African Superswell. We repeated the study by Wang *et al*. (2008), using a different approach to match the waveforms, and obtain a very different result.

We used an iterative technique that utilises a conjugate gradient algorithm to invert the waveforms and to derive our final model. The conjugate gradient algorithm is a local optimisation technique, hence it is dependent on the starting model. If the starting model predicts synthetics that are more than half a cycle different than the data, the inversion can converge to a wrong model, predicting synthetics one cycle off from the data. To solve this problem we derived a top-down solution for our Earth model, where the data most sensitive to the crust and lithospheric mantle was fit first and then the deeper mantle structure was solved for. We also began with longer period filters and then progressively modeled broader band data.

The difference between our model and the model published by Wang *et al*. (2008) is shown in Figure 4.2. Note that the Kalahari model is the average between the Eastern and Central models. Wang *et al*. used SH wave data similar to our data set, but concluded that there is a significant LVZ beneath the Kalahari craton.

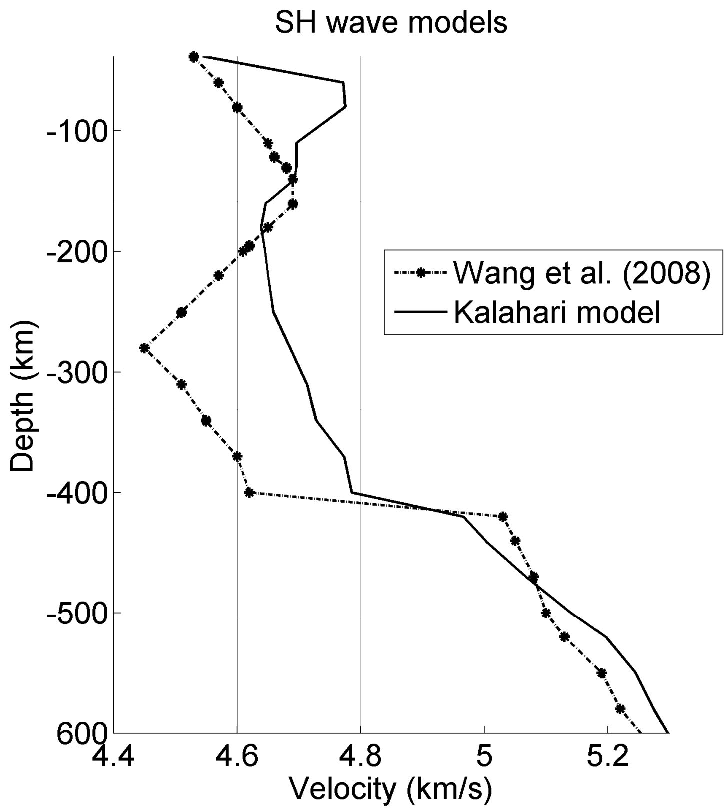

Figure 4.2. Comparison of our preferred SH velocity Kalahari model (solid line), the average between the Eastern and Central models, with Wang* et al.*'s (2008) (dash-dot line with stars) who also used SH body waves.

In Figure 4.3 we compare observed waveforms produced by the M_w=5.9 Lake Tanganyika earthquake with selected synthetics from our Central model, as well as synthetics computed using the Wang *et al*. (2008) model. Both models at these distance ranges produce a first arrival from the high velocity lid (labelled L), a tunnelled turning wave from below the lid (labelled T), lid multiples that are prominent at the short distances, and strong arrivals from the 410 km and 660 km discontinuities. The Wang *et al*. model produces a large arrival from the 410 km discontinuity at a shorter distance than seen in the data (~18°) and also does not fit the timing of the 410 km arrival at larger distances (20° to 21°). The large out-of-phase misfits shown in Figure 4.3 can also be seen in Wang *et al*.'s (2008) publication for all data from 17° to 19°. Although first arrival times can be fit equally well with both models even when using different origin times, we feel that our model provides a better fit to the later arrivals that are most sensitive to the velocities from 200 to 400 km depth. We believe that our staged frequency inversion provides a more robust inversion than trial and error modelling of Wang *et al*. (2008).

We conclude that the difference between our model and Wang *et al.*'s (2008) result is due to different procedures followed during the inversion. We find no flaw in the underlying assumptions of the investigation, nor can the differences be explained by physical factors, such as anisotropy.

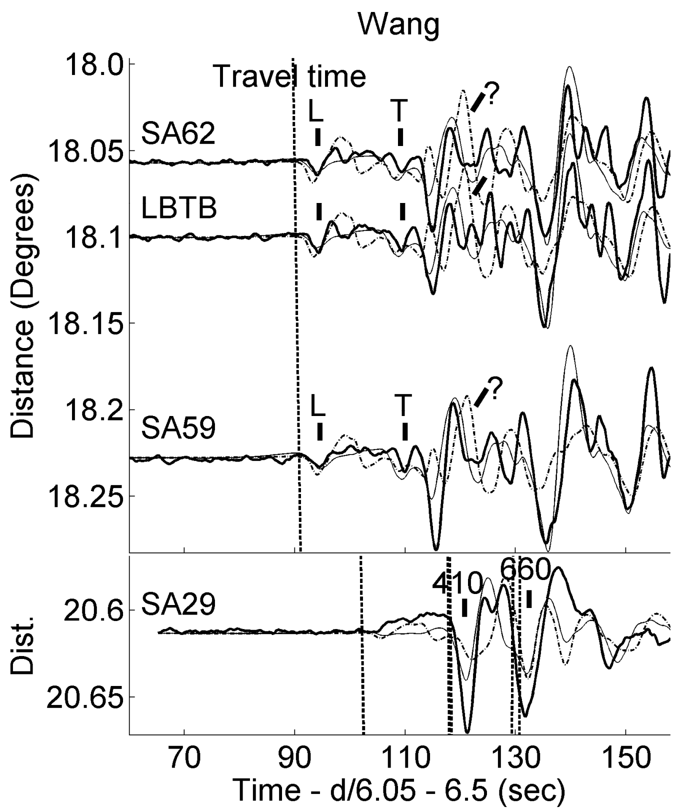

Figure 4.3. Four examples of synthetics computed using Wang* et al.*'s model (2008) (dash-dot lines) compared to the data (heavy lines) and synthetics computed using our Central model (thin lines). The seismograms were integrated to simulate the displacement traces in Wang* et al.*'s publication. Arrivals labelled L travel through the high velocity lid, arrivals labelled T are a tunnelled, turning wave from below the lid, and arrivals labelled 410 and 660 are waves that reflect or turn near the 410 km and 660 km discontinuities, respectively. An unmatched phase is labelled with an "?". Predicted travel-time curves (dashed lines) are overlain on the traces.

4.4 Sensitivity analysis

We estimated uncertainties and non-uniqueness in our final model by running inversions with several different starting models that produce similar fits to the data. In this way we estimated errors in our model due to the earthquake source parameters. We found that differences in source mechanism had little effect on our final models, but errors in origin time, location and depth changed the velocities we found in our inversions. The sensitivity analysis was an important part of our investigation, as it provided deeper insights into the underlying assumptions of the techniques and models, the effect of inversion procedures, the resolution of the velocity structures, and the range of valid models.

Before even starting with the inversions we obtained a source time function and earthquake depth with the waveform data recorded by a station at teleseismic distance on Antarctica. We modelled errors associated with origin time, changes in the 410 km and 660 km transition zone discontinuities and velocity gradient inside the transition zone, as well as assessed the robustness of the slight LVZ. The sensitivity analysis estimated the uncertainties and non-uniqueness of our results. We concluded that the resolution of our model is adequate to exclude a significant LVZ as determined by Wang *et al*. (2008) and that other features of our model are also well resolved. The differences between the models cannot be explained by a lack of resolution.

4.5 The upper mantle Low Velocity Zone

The waves we used to derive our Kalahari model turn in the upper mantle beneath the Zimbabwe craton. Our Kalahari model shows a high velocity lithospheric mantle lid, with the shear velocity beneath the Kalahari craton similar to the velocities found beneath other cratons, and slightly slower velocities in the deep lithosphere (Figure 4.4). The slower velocities in the deep lithosphere may be due to a combination of higher temperatures and, to a lesser extent, chemical alteration due to metasomatism and/or melt infiltration. We found that less than half of the anomalously high elevation of the Kalahari craton can be attributed to buoyancy arising from the deep lithosphere if the seismic anomaly is purely thermal. The Kalahari shear velocity model is consistent with a mantle lithosphere that has an excess temperature of ~90 K over a 110 km thickness, together with an Mg# decrease of ~-2 caused by metasomatism and/or melt infiltration. However, the Mg# decrease cancels out the the buoyancy effect of the 90 K temperature increase. Thus we concluded that deep mantle processes are likely to be the cause of the high elevation of the Kalahari craton, and probably also for the African Superswell, at least across southern Africa.

Our interpretation is very different to that of Li and Burke (2006) and Wang *et al.* (2008), who concluded that high temperature is probably the cause of the LVZ that they found in the upper mantle. They argue that the largest plausible Mg# difference between a fertile (88–89) and a depleted cratonic mantle (92–93) is about five units, which only accounts for a shear wave reduction of 1 to 1.5%, and therefore invoke high temperatures to explain the large velocity drop of 4% in their LVZ.

We note that our investigation only compared body wave velocity models, and recommend that similar comparative studies be performed on the surface wave models.

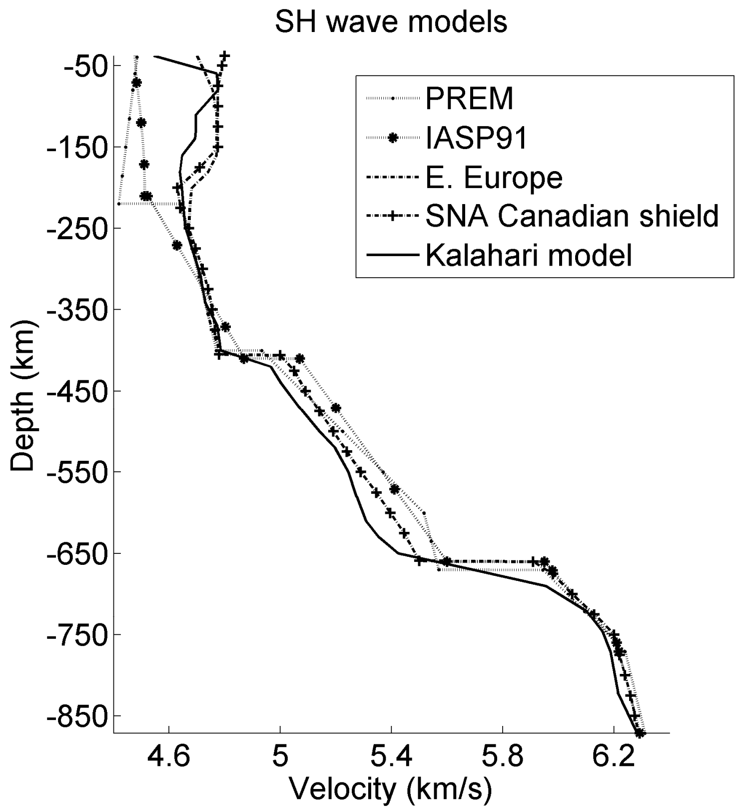

Figure 4.4. Comparison of our preferred SH velocity Kalahari model to the IASP91 model and PREM model. The Kalahari model is also compared to the East European Platform model of Matzel and Grand (2004) and model SNA that was derived from data sampling the Canadian Shield (Grand and Helmberger, 1984).

5. Paper II: Middle mantle seismic structure

5.1 Work done by the PhD candidate

Dr Simmons, former student of the University of Texas at Austin, and now working at the Lawrence Livermore National Laboratory, set up his MatTimes code to pick new S-phases by matching synthetic waveforms with recorded seismograms. I subsequently obtained waveform data from the global network of seismographs as well as AfricaArray stations for 58 earthquakes and added 2600 new phase readings to Grand's global tomography data set.

Prof. Grand provided me with his inversion code. I added a WKBJ algorithm (Chapman, 1978) to calculate ScS travel-times to the forward modelling code to increase the number of phases that traversed the very deep mantle to better image the Superplume at the core–mantle boundary. Afterwards, I executed the tomography inversion code on a powerful SUN workstation and derived an updated global tomography model. One inversion typically lasted 50 minutes. I adapted graphing software, originally written for a SUN workstation, for a LINUX PC and produced all the cross-sections and depth slices. I then modified the inversion code to set to zero the perturbations of small "obstruction volumes" in the 3D tomography model. Afterwards, I repeated the inversions with the modified code to prepare the travel-time residuals of the reference global model and the modified global models (with obstruction volumes) for various hypotheses tests. Testing for a hypothesis with different smoothing was run overnight.

I developed the hypothesis testing procedure, wrote the Matlab code for a Windows PC, executed all the F-tests, and produced all the graphs. I wrote this paper. At the time the thesis was examined, the paper was being reviewed by the journal Pure and Applied Geophysics.

5.2 Previous models

Ritsema *et al*., 1999 proposed that the African Superplume extends from the core–mantle boundary under southern Africa into the slow-velocity anomaly in the upper mantle under eastern Africa. (Figure 5.1a). Subsequently several other global tomography studies (e.g., Ritsema and Van Heijst, 2000; Grand, 2002; Montelli *et al*., 2006) visually interpreted what seem to be weak connections between the upper slow velocity anomaly and the lower African Superplume. Grand's (2002) tomographic model images show slow shear velocities associated with the East African Rift from the surface to a depth of at least 325 km. At greater depth, several slow-velocity arms extend westwards and southwards from the Rift towards the West African Craton where, at greater depths, these arms join and link with the top of the African Superplume (Begg *et al*., 2009). The tomography images of Montelli *et al*. (2006)

show two isolated slow-velocity anomalies beneath the Horn of Africa, one located beneath the Afar triple junction (42° E, 12° N), and the other beneath the Tanzanian craton (32° E, 3° S) (Figure 5.1b). Their shear wave image shows a weak connection below 650 km between the anomaly beneath Tanzania, which dips westwards, and with the top of the African Superplume. A connection between the slow-velocity anomaly underneath Afar dipping southwest towards the African Superplume is also weakly defined. The connection of the anomaly beneath Lake Victoria with the African Superplume is more clearly visible (Figure 5.1b).

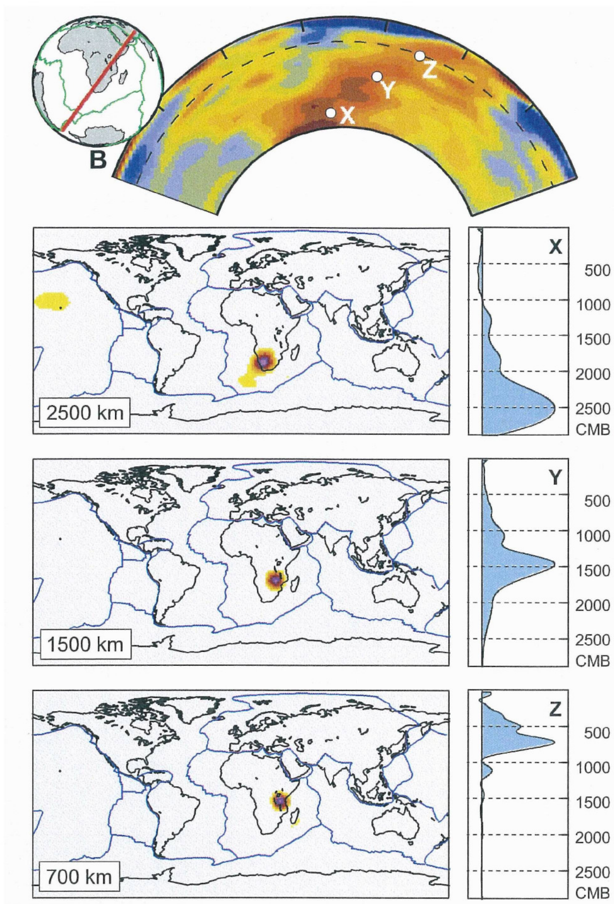

Figure 5.1a. Backus-Gilbert resolution kernels for locations X, Y and Z at 2500, 1500 and 700 km depth, respectively, in the mantle beneath Africa. Horizontal cross-sections through the Backus-Gilbert kernels are shown on the left. The relative amplitude of the kernels (from 0.1 to 1.0) is represented by nine colors, which range from yellow to red to pink. Regions where the Backus-Gilbert kernels have a relative amplitude lower than 0.1 are not shaded. The radial dependence of the kernels is shown on the right (After Figure 4 in Ritsema **et al.**, ***1999).***

Whereas Montelli *et al*. (2006) state that the lower mantle image of Afar is not an effect of leakage (Figure 5.1b), Ritsema *et al*. (1999) are the only researchers who quantify their result. They investigated the weakening of the slow-velocity anomaly between 670 and 1000 km depth with an application of Backus-Gilbert resolution kernels (Figure 5.1a). This led them to conclude that the continuity of the slow-velocity anomaly at 2500, 1500 and 700 km depths is not caused by preferential SW–NE body-wave sampling. Whether the slow-velocity anomaly in the upper mantle is indeed connected to the deeper Superplume or whether these weak connections are only leakages, is not clear.

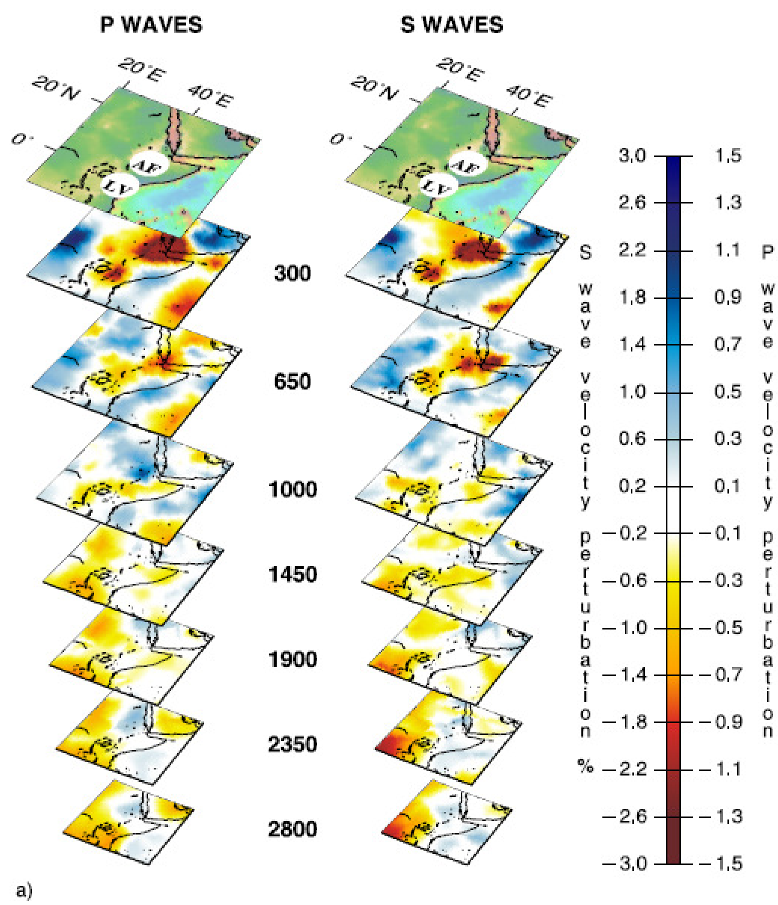

Figure 5.1b. Three-dimensional view of the plumes beneath the horn of Africa: AF (Afar) and LV (Lake Victoria) in both (left) P-wave and (right) S-wave tomographic models. Cross-sections are 40° by 40° centred around the studied plume. The vertical scale has been exaggerated to avoid overlapping of the sections (After Figure 12a in Montelli* et al.*, 2006).

5.3 Statistical hypothesis testing

Our objective is to investigate rigorously the evidence for a connection between the African Superplume and the upper mantle anomaly beneath East Africa. We perform statistical tests to compare two end-member models: (i) a model where the upper slow-velocity anomaly is linked in a complex way to the Superplume, and (ii) a model where the upper anomaly is not connected to the Superplume. The tomographic model is derived as before. For the hypotheses testing we construct models where the upper- and lower mantle anomalies are separated by various regions of average mantle slowness between 670–1000 km depth. We name these regions "obstruction volumes", following the suggestion of Montelli *et al.* (2004) that a thermal boundary layer divides the mantle into two convecting regions, which are linked in a complex way, unlike the simple models of either whole or layered mantle convection. Our model-naming convention is that BLOCK-N refers to a model where the slowness anomaly is constrained to be zero in a volume in the N^{th} shell from the Earth's surface.

We perform an F-test to objectively assess the evidence for complex, weak connections through the middle mantle. Our statistical tests do not rely on a visual interpretation of tomographic images that are dependent on the image processing techniques such as the amount of smoothing. Rather, the statistical test gives an objective decision on the probability that a hypothesis is true. Previous procedures for estimating reliability and resolution in tomographic models include synthetic inversions with random travel-time errors and synthetic inversions on data with travel-time residuals corresponding to a given pattern of mantle heterogeneity, the so-called "checkerboard" tests (e.g., Grand, 1994). Even these tests, though, depend on the image processing procedures.

Table 1 summarises the various test models and the results are shown in Figure 5.2. The statistical null hypothesis is the model where the Superplume penetrates through the middle mantle (Begg *et al.*, 2009). At a smoothing weight of 20, test models BLOCK-09-10-11 and BLOCK-10 have probabilities of being valid of 31.8% and 50.1%, respectively (Figure 5.2). Our statistical testing indicates that the alternative hypothesis, which has a "obstruction volume" of a mere 150 km thickness, fits the data as well as the REFERENCE model (null hypothesis) with a connection between the deep mantle and upper mantle slow velocities regions. We repeated our tests with various smoothing parameters (1, 10, 20, 60 and 120) and determined that smoothing does not adversely affect our hypothesis testing. A complete description of the testing may be found in Paper II.

Table 1
Volume thickness of the BLOCK models

Test model	Depth	Comment	Result
BLOCK-06-07	400–650 km	Mantle transition zone	False
BLOCK-08	650–750 km	Thin upper mantle	False
BLOCK-07-08-09	525–850 km	Medium upper mantle	False
BLOCK-06-07-08-09-10	400–1000 km	Thick upper mantle	False
BLOCK-10	850–1000 km	Thin middle mantle	Equal probability false and true
BLOCK-09-10-11	750–1150 km	Medium middle mantle	False
BLOCK-08-09-10-11-12	650–1300 km	Thick middle mantle	False
BLOCK-12-S	1150–1300 km	Thin lower mantle	False
BLOCK-11-12-13-S	1000–1450 km	Medium lower mantle	False
BLOCK-10-11-12-13-14-S	850–1600 km	Thick lower mantle	False
BLOCK-13-14	1300–1600 km	Test for volume limit sensitivity	False
BLOCK-13-14-S	1300–1600 km	Test for volume limit sensitivity	False

The postscript S in model names refers to deep tests between 850 and 1600 km and with a different lateral extent.

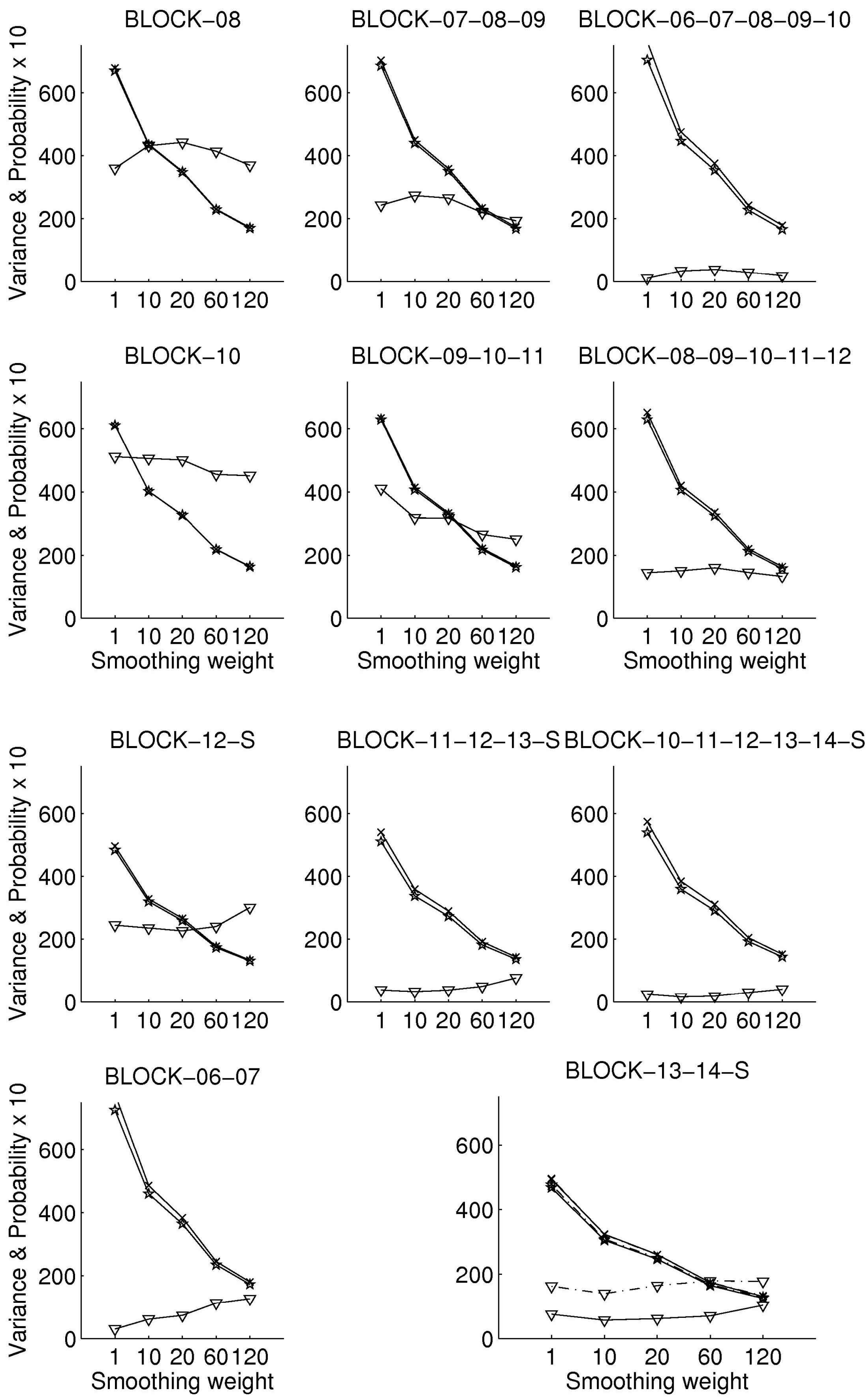

Figure 5.2. Variances for the respective reference models (stars) and BLOCK models (crosses) and probability at 5% significance ×10 (triangles) as a function of the central smoothing weight.

5.4 The connection through the middle mantle

Our result agrees with that of Ritsema *et al*. (1999), namely that the Superplume could be weak in the middle mantle, but differs in that we find a very thin weak zone rather than a broad weakening between 670 and 1000 km depth (Figures 5.3a and 5.3b). We conclude that the African Superplume rises to at least 1150 km depth (more likely to 1000 km) and that the shallow slow-velocity anomaly continues from the surface to below the mantle transition zone. However, the relatively small thickness of the "obstruction volume" (of only 150 km) and the dynamic, high topography of the African Superswell (Lithgow-Bertelloni and Silver, 1998) argue against a complete separation of the mantle into two convecting regions, in accord with the model Montelli *et al*. (2004) developed from an interpretation of a global catalogue of plumes.

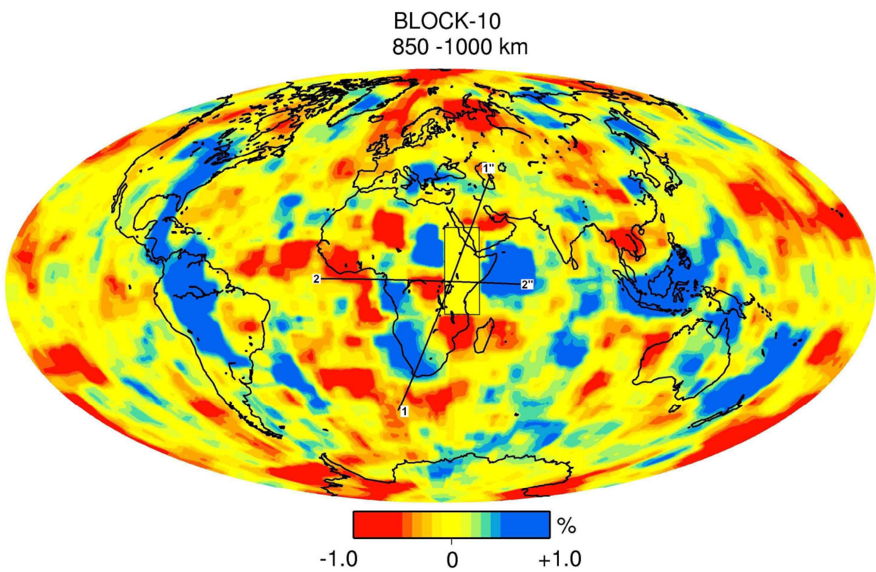

Figure 5.3a. Shell from model BLOCK-10 at 850–1000 km depth smoothed with a central weight of 20. The volume with the velocity perturbation constrained to zero during the inversions is indicated with a yellow block beneath eastern and southern Africa. The volume constrained during the whole mantle inversion is indicated in black on cross-section 1.

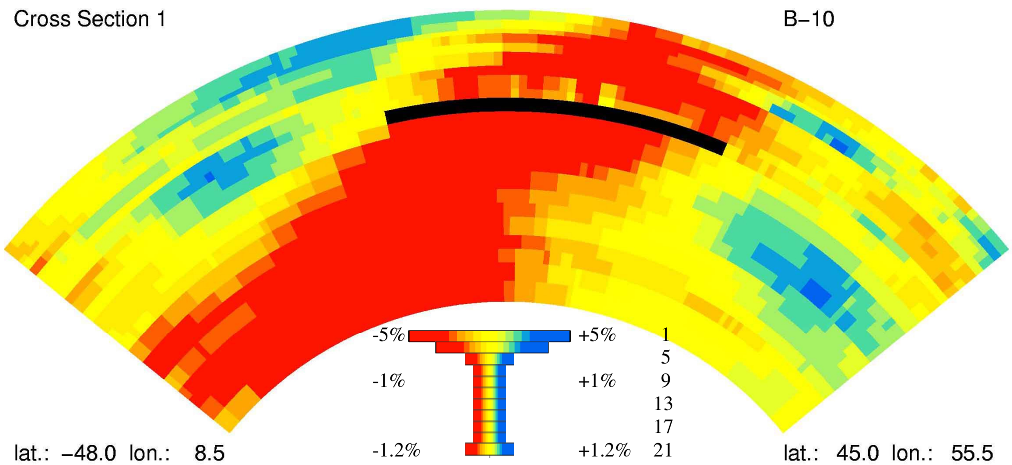

Figure 5.3b. Cross-section 1 for model BLOCK-10 smoothed with a central weight of 20. The volume with the velocityperturbation constrained to zero during the whole mantle inversion is indicated in black. A relative scale is shown at the bottom for every second layer with every 4th layer numbered: below 650 km and above 2500 km depth the scale is the same for all the layers.

6. Paper III: Study of regional moment tensors

6.1 Work done by PhD candidate

I derived the new regional moment tensors in publication III with software provided to me upon request by Prof. Dreger from the University of California, Berkeley, USA. I re-compiled the FORTRAN source code without modification, installed it on a LINUX computer and tested the software with the examples provided.

I searched the seismological bulletins of the Council for Geoscience for earthquakes of magnitude 3.5 and larger for the period that the Kaapvaal craton array was operational. I obtained the corresponding waveform data for 37 suitable earthquakes from the IRIS PASSCAL data centre. I used the spectral analysis module of the SAC software to narrow this down to three earthquakes recorded by at least five stations with an adequate S/N ratio. Afterwards I completed the inversions to derive the moment tensors. One inversion took about one minute of computer time.

I wrote the article. Mr. Ian Saunders calculated the fault plane solution and determined the depth from P_n, P_g, S_n, and S_g phases.

6.2 Stress patterns and surface uplift

The large-scale slow shear wave velocity anomaly beneath the African plate can be interpreted as mantle flow induced by density variations that can dynamically support the excess elevation of the African Superswell (Lithgow-Bertelloni and Silver, 1998). Not only eastern Africa, but also southern Africa is being actively uplifted; Southern Africa at a rate of at least 8 to 17 m/Myr (Gurnis *et al*., 2000) (Figure 6.1). This differs from the first-order global stress patterns in the lithosphere presented by Zoback (1992) where ridge push (strike-slip stress regime) dominates the whole of southern Africa, and only in the East African Rift the buoyancy force (normal faulting regime) overcomes the compression due to ridge push. Normal faulting associated with the Rift extends as far south as Mozambique (e.g., Yang and Chen, 2008). We hypothesise that normal faulting due to the active uplift of southern Africa (Gurnis *et al*., 2000) should extend into the northern regions of South Africa (e.g., Fan and Wallace, 1995).

Fault mechanisms have been rarely studied in South Africa because of the low level of natural seismicity. However, frequent small- to medium-sized earthquakes related to South Africa's deep gold mining activities occur in northeastern South Africa (e.g., Saunders *et al*., 2008). The largest principle stresses in the Savuka mine in the Far West Rand gold-mining area are compressive, orientated near vertically, and relaxed through a mix of volume closure and normal faulting for earthquakes with $0.5 < M_w < 2.6$ (Julià *et al*., 2009). Hence, our analysis of selected mine-related earthquakes of

M_w ~4 may provide valuable information about the regional stress field when calculating moment tensors, provided that the faulting component dominates the mine-related volume closure.

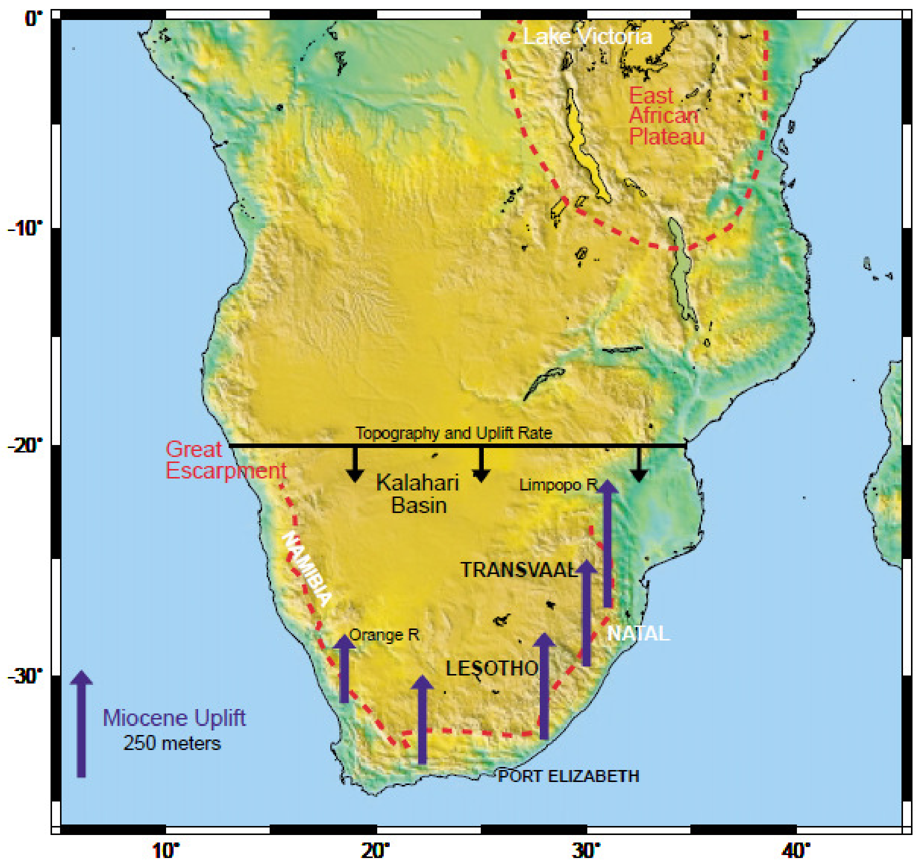

Figure 6.1. Shaded relief map of southern Africa. The approximate position of the Great Escarpment and Miocene uplift are indicated. A total uplift of 250 m has been determined by Partridge and Maud (1987) for the continental region below the "Topography and Uplift Rate" line. Gurnis* et al. *(2000) constrained their mantle dynamic topography models with this uplift rate (after Figure 2 in Gurnis* et al.*, 2000).

6.3 Sparse available tensors

Earthquakes from the South African National Seismograph Network (SANSN) and historic databases with M_L larger and equal to 4 for the period 1620 to 2009 are shown in Figure 6.2. Tremors resulting from the deep mine operations in the gold fields, e.g. 1, 2, E and F form the bulk of the seismic events recorded by the SANSN. Previously published focal mechanisms/moment tensors are plotted as "beach balls" A to F. We derived new regional moment tensors (RMTs) for earthquakes 1, 2 and 3.

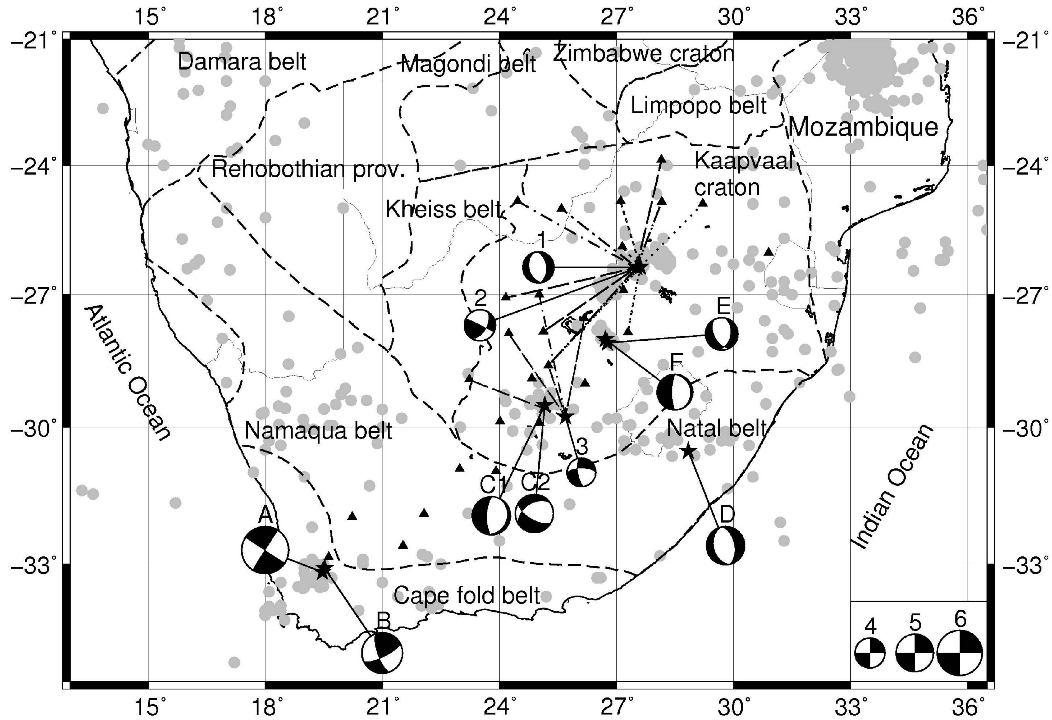

Figure 6.2. Location map of the seismic stations and earthquakes used in this study. Black stars represent the epicentres and triangles the stations. Moment tensors/fault plane solutions are indicated with "beach balls" with sizes proportional to magnitude. Previous solutions are marked with letters A to F and new moment tensors by numbers 1 to 3. Dotted and dash-dot lines show where waves propagate between earthquakes 1 to 3 and the stations used for the moment tensor inversions; other stations were used for the fault plane solution. Major tectonic provinces are separated with thick dashed lines and are labelled. Earthquakes from 1620 to 2009 with local magnitude larger than and equal to 4 are plotted with grey dots.

6.4 New moment tensors

1997-09-25 Far West Rand gold mines

The derived focal mechanism and stress directions are consistent with previous solutions for earthquakes D, E and F. All these solutions were produced in an east–west principle extensional stress system. Our solution compares well with the normal faulting regime for Savuka mine found by Julià *et al*. (2009), but without the volume closure. There is a discrepancy between M_L=4.5 and the calculated M_w=4.1 for this event. The next two solutions will show that differences between M_L and M_w are a recurring issue for South Africa.

1998-12-05 Far West Rand gold mines

We derived an oblique strike slip focal mechanism with the P-axis in the north-northwest direction and the T-axis towards the west-southwest. The derived focal mechanism differs from previous solutions D, E and F, as well as the normal faulting regime for Savuka mine found by Julià *et al*. (2009). The decomposition of the solution into 53% major versus 47% minor double couple indicates the source could have a significant percentage volume closure, as was found by Julià *et al*. (2009) for smaller magnitudes. Again, there is a discrepancy between the calculated M_L=4.3 and M_w=4.1 for this event.

1999-02-04 Fauresmith area in the Koffiefontein cluster

We derived a double-couple oblique normal fault focal mechanism with the P-axis dipping towards the southeast and the T-axis in the southwest direction. A depth of 11 km yields the largest variance reduction between the observed and synthetic waveforms and the highest double-couple percentage. The derived focal mechanism and stress orientation differ from previous solutions C1 and C2 derived for earthquake C (Figure 6.1). Again, there is a discrepancy between the magnitudes (M_L=4.5 as opposed to M_w=3.8) for this event.

6.5 Implications for the crustal stresses regime

The stable Kalahari craton might experience subtle heating and uplift owing to lithospheric modification at its base and/or the African Superplume (Papers I and II). The faulting regime in southern Africa changes from normal faulting (extension) in the northeast near the East African Rift to strike-slip faulting in the southwest (Figure 6.2). We interpret the moment tensors/focal mechanisms as: (1) In northeastern South Africa, solutions are the result of crustal stresses associated with uplift/rifting, even though the higher seismicity associated with the East African Rift does not extend into the country. Stresses related to deep mining operations modify the normal faulting regime causing local volume closures; (2) Earthquake C with conflicting solutions C1 and C2 and different RMT No. 3 are situated at the change-over area to (3) southwestern South Africa, where ridge push from the surrounding plate boundaries and/or local crustal thicknesses determine the stress regime. This confirms the hypothesis of stress patterns that can be related to the surface uplift of southern Africa.

7. Summary of papers and proposed future work

7.1 Paper I: S-velocity seismic structure of the upper mantle

We present new one-dimensional SH-wave velocity models of the upper mantle beneath the Kalahari craton in southern Africa obtained from waveform inversion of regional seismograms from an M_w = 5.9 earthquake located near Lake Tanganyika recorded on broadband seismic stations deployed during the 1997–1999 Southern African Seismic Experiment. The velocity in the lithosphere beneath the Kalahari craton is similar to that of other shields, and there is little evidence for a significant low velocity zone beneath the lithosphere. The velocity of the lower part of the lithosphere, from 110 to 220 km depth, is slightly slower than beneath other shields, possibly due to higher temperatures or a decrease in Mg number (Mg#). If the slower velocities are caused by a thermal anomaly, then slightly less than half of the unusually high elevation of the Kalahari craton can be explained by shallow buoyancy from a hot lithosphere. However, a decrease in the Mg# of the lower lithosphere would increase the density (fertile Mg# 88–89 has higher density and craton/depleted Mg# 92–93 has lower density) and counteract the buoyancy effect of the higher temperatures. We obtain velocity jumps of between 0.16 ± 0.1 and 0.21 ± 0.1 km/s across the 410 km discontinuity. We also obtain a thickness of 250 ± 30 km for the mantle transition zone, which is similar to the global average, but the velocity gradient between the 410 and 660 km discontinuities is less steep than in global models, such as PREM and IASP91. Our results suggest that there may be a thermal or chemical anomaly in the mantle transition zone. Overall, our seismic models provide little support for an upper mantle source of buoyancy for the unusually high elevation of the Kalahari craton, and hence the southern African portion of the African Superswell.

7.2 Paper II: Middle mantle seismic structure

We present the results of statistical hypothesis testing of a global tomography model of three-dimensional shear velocity variations for the middle mantle beneath eastern and southern Africa. We apply an F-test to evaluate the validity of a model where a tilted, slow-velocity anomaly in the deepest mantle under southern Africa, known as the African Superplume, is continuous with a slow-velocity anomaly in the upper mantle under eastern Africa. This null hypothesis is tested against alternative hypotheses in which various “obstruction volumes” in the middle mantle are constrained to zero velocity perturbation with respect to the one-dimensional reference model during the tomographic inversion. I found that a model with a thin “obstruction volume” at 850–1000 km depth fits the data as well as a model with a continuous slow-velocity anomaly. Models with obstruction volumes at other depths are rejected. We conclude that the African Superplume rises to at least 1150 km depth and that the upper mantle slow-velocity anomaly continues from the surface to below the mantle transition zone. We interpret the "obstruction volume" as a weakening of the Superplume in the middle mantle.

7.3 Paper III: Study of regional moment tensors

Regional moment tensors (RMTs) provide important information for seismotectonic and hazard studies in regions with low to moderate seismicity, where infrequent earthquakes of $M_w \geq \sim 4.0–4.5$ occur that are too small for global moment tensor techniques. Moment-tensor analysis involves fitting theoretical waveforms with observed broadband waveforms and inverting for the moment-tensor elements. One powerful tool to calculate RMTs is the time domain surface wave waveform inversion code TDMT_INVC (Dreger 2003). In recent years RMTs have been routinely calculated with this software in many parts of the world such as western Canada, California, Alaska, Japan, Taiwan, the European–Mediterranean region, and New Zealand.

Only a few moment tensors/focal mechanisms are available for South Africa. This is due to moderate tectonic and deep mine-related seismicity, as well as, until recently, a sparse distribution of broadband seismometers in the South African National Seismograph Network (SANSN). A unique opportunity presented itself when the dense, very broadband Southern African Seismic Experiment Kaapvaal craton array was deployed in South Africa. From this array we identified three near regional M_w ~4.0 earthquakes with suitable waveform data to calculate RMTs with the TDMT_INVC software. Our goal is to determine the moment magnitude, earthquake mechanism, and focal depth in order to 1) make progress in resolving the difference between local and moment magnitudes routinely determined with the SANSN; and 2) expand our understanding of the regional seismotectonics and deep mine-related earthquakes.

In this article we first review the regional seismotectonics and SANSN routine earthquake location procedures. Next, we select appropriate velocity and attenuation models as input for the TDMT_INVC software, invert three earthquake waveforms, and complete a sensitivity analysis to estimate the reliability of the three solutions. Then we interpret the results with the seismotectonics. We also discuss our future plans to calculate moment magnitudes for the SANSN and derive an M_L–M_w relationship.

7.4 Implications for the structure and evolution of the mantle beneath southern Africa and proposed future work

The study of Earth structure and earthquake sources in southern and eastern Africa is influenced by a single massive lower mantle structure (the African Superplume), which may be connected to the shallow, slow-velocity anomaly under eastern Africa associated with the East African Rift System (EARS). The African Superswell is a broad region of elevated topography roughly coincident with the Superplume. The cause of the uplift, which occurred in during the last 20 Ma or so, has been the subject of much research and debate. It is likely that the East African plateau is related to the EARS upwelling. This has led researchers to speculate that there is a source of buoyancy in the upper mantle beneath the southern African plateau. However, the various investigations of the upper mantle seismic structure by Priestly (1999), Saltzer (2002), Larson *et al*. (2006), Li and Burke (2006) and Wang *et al*. (2008) have produced very different results. Some studies find evidence for a very strong LVZ, a plausible source of shallow mantle buoyancy, whereas others have found only a slight LVZ. We repeated the investigation by Wang *et al*. (2008), to determine the reason for the different results. In our opinion there is no flaw in the underlying assumptions of Wang *et al*.'s investigation, nor can the differences be explained by physical factors, such as anisotropy. The resolution and range of results is adequate to map the upper mantle structure and estimate the amount of buoyancy. Our conclusion is that the differences are a result of the choice of inversion method and procedure. Our study only concentrated on one model using SH body waves. We recommend that the surface wave results should also be re-calculated using different inversion algorithms and procedures.

If the Superplume is indeed connected to the shallow velocity anomaly under eastern Africa, then the Superplume may play an important role in the volcanism and rifting associated with the East African Rift. However, previous studies rely on a visual interpretation of tomographic images. Since these images depend on the imaging procedure (e.g., the amount of smoothing), it is difficult to evaluate the evidence for a complex connection through the middle mantle. Our approach is to use a statistical hypothesis test to objectively determine the probability that a hypothesis is true or false for both interpretations, namely, the existence/non-existence of such a connection. Our result shows that both models could be true with equal probability. This highlights the obvious need for more data to better image the African Superplume. The testing procedure relied on separating the upper and lower mantle anomalies by setting to zero the velocity perturbation (from the one-dimensional reference model), for the volume between them. Unfortunately, the present, modified inversion algorithm does not allow for testing a forced connection through the middle mantle, even though this alternative hypothesis test might be very useful to further investigate the tenuous connection. We suggest that the modified inversion algorithm be further developed to test for such a case.

The uplift of southern Africa has led researchers to propose that the buoyancy, associated with the East African Rift, also uplifts southern Africa. If so, then the ridge push from the surrounding spreading plate boundaries would only dominate the south of South Africa. Three new moment tensors have been derived: one for a tectonic earthquake, and two for mine-related earthquakes. If the regional stress field can be obtained from the mine-related earthquakes in addition to the volume closure components, then our results confirm the hypothesis that the northern part of South Africa is being uplifted owing to lithospheric modification at its base and/or the African Superplume. However, moment tensors and focal mechanisms for South Africa are sparse and hence more earthquakes must be analysed to further interpret the stress pattern in South Africa associated with the African Superplume.

Acknowledgements

I wish to thank my study advisor, Prof. Grand, from whom I learned that “more and faster does not always lead to better”. His obsession with quality data, detailed interpretation, deep understanding, thorough testing, impeccable research procedures, and an uncompromising attitude towards detail has both guided and inspired me.

Dr Eric Matzel kindly took the time to discuss his inversion software with me by e-mail when I started out with the upper mantle seismic structure.

Many thanks to Dr Simmons for setting up his MatTimes code, his advice at the beginning of my research on accurate S-phases picking and highlighting pitfalls and suggesting procedures that set me on my way.

I also wish to thank Prof. Dreger whom I never met but who immediately upon request provided me with his Time Domain Regional Moment Tensor Inversion software for my research.

Ass. Prof. Ottemöller suggested changes to the early draft manuscript of the moment tensor paper and I am thankful for that.

Finally, I wish to thank Prof. Nyblade, co-director of the AfricaArray programme and student graduate co-ordinator Prof. Durrheim, for the opportunity to visit the University of Texas at Austin four times over the summer semesters of 2006–2009 for collaborative research.

The Council for Geoscience supported me with a bursary and kindly allowed me to take study leave from my normal work duties.

Language editing was done by Beverlie Davies and Sonja van Eck.

References

Begg, G. C., W. L. Griffin, L. M. Natapov, S. Y. O' Reilly, S. P. Grand, C. J. O' Neill, J. M. A. Hronsky, Y. Poudjom Djomani, C. J. Swain, T. Deen, and P. Bowden, (2009), The lithospheric architecture of Africa: Seismic tomography, mantle petrology, and tectonic evolution, *Geopsphere*, *5*, 23-50.

Bina, C. R., and G. Helffrich (1994), Phase transition Clapeyron slopes and transition zone seismic discontinuity tomography, *Journal of Geophysical Research*, *99*, 15,853-15,860.

Chapman, C. H. (1978), A new method for computing synthetic seismograms, *Geophysical Journal of the Royal Astronomical Society*, *5*, *4*, 481–518.

Dreger, D. S. (2003). TDMT_INVC: Time domain seismic moment tensor INVersion. In *International Handbook of Earthquake and Engineering Seismology*, ed. W. H. K. Lee, 81B, 1,627. Boston: Academic Press.

Dziewonski, A. M., and D. L. Anderson (1981), Preliminary reference Earth model, *Physics of the Earth and Planetary Interiors*, *25*, 297–356.

Dziewonski, A. M. (1984), Mapping the lower mantle: Determination of lateral heterogeneity in P velocity up to degree and order 6, *Journal of Geophysical Research*, *89*, 5929–5952.

Fan, G., and T. Wallace (1995), Focal mechanism of a recent event in South Africa: A study using a sparse very broadband network, *Seismological Research Letters*, *66*, 13-18.

Gao, S. S., P. G. Silver, and K. H. Liu (2002), Mantle discontinuities beneath Southern Africa, *Geophysical Research Letters*, *29*, 1291-1294.

Grand, S. P., and D. V. Helmberger (1984), Upper mantle shear structure of North America, *Geophysical Journal of the Royal Astronomical Society*, *76*, 399-438.

Grand, S. P. (1994), Mantle shear structure beneath the Americas and surrounding oceans, *Journal of Geophysical Research*, *99*, B6, 11,591–11,621.

Grand, S. P. (2002), Mantle shear-wave tomography and the fate of subducted plates, *Philosophical Transactions of the Royal Society of London*, *360*, 2475–2491.

Gurnis, M., J. X. Mitrovica, J. E. Ritsema, and H. –J. Van Heijst (2000), Constraining mantle density structure using geological evidence of surface uplift rates: The case of the African Superplume, *Geochemistry Geophysics Geosystems*, *1(7)*, doi:10.1029/1999GC000035.

James, D. E., M. J. Fouch, J. C. VanDecar, S. van der Lee, and Kaapvaal Seismic Group (2001), Tectonospheric structure beneath southern Africa, *Geophysical Research Letters*, *28*, 13, 2485-2488.

Julia, J., A. A. Nyblade, R. Durrheim, L. Linzer, R. Gok, P. Dirks, and W. Walter (2009), Source mechanisms of mine-related seismicity, Savuka mine, South Africa, *Bulletin of the Seismological Society of America* 99, 2,801-2,814.

Larson, A. M., A. Snoke, and D. E. James (2006), S-wave velocity structure, mantle xenoliths, and the upper mantle beneath the Kaapvaal craton, *Geophysical Journal International*, *167*, 171-186, doi:10.1111/j.1365-246X.2006.03005.x.

Lay, T., and T. C. Wallace (1995), Modern global seismology, *Academic Press, San Diego, California, USA*, 521 pp.

Li, A., and K. Burke (2006), Upper mantle structure of Southern Africa from Rayleigh wave tomography, *Journal of Geophysical Research*, *111*, B10303, doi:10.1029/2006JB004321.

Lithgow-Bertelloni, C., and P. G. Silver (1998), Dynamic topography, plate driving forces and the African superswell, *Nature*, *395*, 269-272.

Matzel, E., and S. P. Grand (2004), The anisotropic seismic structure of the East European platform, *Journal of Geophysical Research*, *109*, B01302, doi:10.1029/2001JB000623.

Montelli, R., G. Nolet, F. A. Dahlen, G. Masters, E. R. Engdahl, and S. Hung (2004), Finite-frequency tomography reveals a variety of plumes in the mantle, *Science*, 303, 338–343.

Montelli, R., G. Nolet, F. A. Dahlen, and G. Masters (2006), A catalogue of deep mantle plumes: New results from finite-frequency tomography. *Geochemistry Geophysics Geosystems*, *7*, Q11007, doi:10.1029/2006GC001248.

Moucha, R., and A. M. Forte (2011), Changes in African topography driven by mantle convection, *Nature geoscience*, *4*, 707-712.

Ni, S., E. Tan, M. Gurnis, and D. Helmberger (2002), Sharp sides to the African Superplume, *Science*, *296*, 1850–1852.

Ni, S., D. V. Helmberger., and J. Tromp (2005), Three-dimensional structure of the African superplume from waveform modeling, *Geophysical Journal International*, *161*, 283–294.

Nyblade, A., and C. A. Langston (1998), Upper mantle P wave velocities beneath Southern Africa and the origin of the African Superswell, *Southern African Geophysical Review*, *2*, 55–61.

Nyblade, A., and S. Robinson (1994), The African Superswell, *Geophysical Research Letters*, *21*, 765–768.

Nyblade, A. A., T. J. Owens, H. Gurrola, J. Ritsema, and C. A. Langston (2000), Seismic evidence for a deep upper mantle thermal anomaly beneath east Africa, *Geology*, *28*, 599-602.

Nyblade, A., P. Dirks, R. Durrheim, S. Webb, M. Jones, G. Cooper, and G. Graham (2008), AfricaArray: Developing a geoscience workforce for Africa's natural resource sector, *The Leading Edge*, October, 1358-1361.

Partridge, T. C., and R. R. Maud (1987), Geomorphic evolution of southern Africa since the Mesozoic, *South African Journal of Geology*, *90*, 179-208.

Priestley, K. (1999), Velocity structure of the continental upper mantle: evidence from Southern Africa, *Lithos*, *48*, 45-56.

Ritsema, J, S. Ni, D. V., Helmberger, and H. P. Crotwell (1998), Evidence for strong shear velocity gradients in the lower mantle beneath Africa, *Geophysical Research Letters*, *25*, 4245–4248.

Ritsema, J., H. J. van Heijst, and J. H. Woodhouse (1999), Complex shear wave velocity structure imaged beneath Africa and Iceland, *Science*, *286*, 1925-1928.

Ritsema, J., and H. Van Heijst (2000), New seismic model of the upper mantle beneath Africa, *Geology*, *28*, 63–66.

Saltzer, R. (2002), Upper mantle structure of the Kaapvaal craton from surface wave analysis – a second look, *Geophysical Research Letters*, *29(6)*, doi:10.1029/2001GL013702.

Saunders, I., M. B. C. Brandt, J. Steyn, D. L. Roblin, and A. Kijko (2008), The South African National Seismograph Network, *Seismological Research Letters* 79, 203–210.

Silver, P. G., M J. Fouch, S. S. Gao, and M. Schmitz (2004), Seismic anisotropy, mantle fabric, and magmatic evolution of Precambrian Southern Africa, *South African Journal of Geology*, *107*, 45–58.

Simmons, N. A., A. M. Forte, and S. P. Grand (2007), Thermochemical structure and dynamics of the African superplume, *Geophysical Research Letters*, *34*, L02301, doi:10.1029/2006GL028009.

Steinberger, B., and T. H. Torsvik (2010), Towards and explanation for the present and past locations of the poles, *Geochemistry Geophysics Geosystems*, *11*, Q06W06, doi:10.1029/2009GC002889.

Wang, Y., L. Wen, and D. Weidner (2008), Upper mantle SH- and P-velocity structures and compositional models beneath Southern Africa, *Earth and Planetary Science Letters*, *267*, 596-608.

Yang, Z., and W. Chen (2008), Mozambique earthquake sequence of 2006: High-angle normal faulting in southern Africa, *Journal of Geophysical Research*, *113*, B12303, doi:1029/2007JB005419.

Zoback, M. L. (1992), First- and second order patterns of stress in the lithosphere: The world stress map project, *Journal of Geophysical Research*, *97*, B8, 11,703-11,728.